UDC 621.371
doi:10.31799/1684-8853-2018-5-94-103

Surveys

Evolution of multiple-access networks — cellular and non-cellular — in historical perspective. Part 2

A. M. Sergeev[a], Senior Lecturer, orcid.org/0000-0002-4788-9869
N. Sh. Blaunstein[b, c], Dr. Sc., Phys.-Math., Professor, nathan.blaunstein@hotmail.com
[a]Saint-Petersburg State University of Aerospace Instrumentation, 67, B. Morskaia St., 190000, Saint-Petersburg, Russian Federation
[b]Ben-Gurion University of the Negev, POB 653, 1, Ben-Gurion St., Beer-Sheva, 74105, Israel
[c]Jerusalem College of Technology — Lev Academic Center, 21 Havaad Haleumi, POB 16031, Jerusalem, 91160, Israel

Introduction: *The goal of this issue is the analysis of evolution of the current and novel wireless networks, from second generation (2D) to fifth generation (5G), as well as changes in technologies and their corresponding theoretical background and protocols — from Bluetooth, WLAN, WiFi and WiMAX to LTE, OFDM/OFDMA, MIMO and LTE/MIMO advanced technologies with new hierarchy of cellular maps design — femto/pico/micro/macro.* ***Methods:*** *We use new theoretical frameworks for description of the advanced technologies, such as multicarrier diversity technique, OFDM and OFDM novel approach, MIMO aspects description based on multi-beam antennas approach, various cellular maps design based on a new algorithms of femto/pico/micro/macrocell deployment, and a new methodology of a new MIMO/LTE system integration based on multi-beam antennas.* ***Results:*** *We have created a new methodology of multi-carrier diversity description for novel multiple-access networks, of usage of OFDM/OFDMA modulation to obey inter-user and inter-symbol interference in multiple-access networks, of how to obey the multiplicative noises occurring in the multiple-access wireless networks, caused by multi-ray phenomena, and finally, of how to overcome propagation effects occurring in the terrestrial communication links by use combination of MIMO and LTE technologies based on multi-beam antennas. For these purposes we present new stochastic approach that accounts for the terrain features, such as buildings' overlay profile, buildings' density around the base station and each user antennas, and so forth. These parameters allow us to estimate for each situation occurs at the built-up terrain area the effects of fading, as a source of multiplicative noise.* ***Practical relevance:*** *New methodology of how to estimate effects of multiplicative noise, inter-user and inter-symbol interference, occurring in the terrestrial wireless networks, allows us to predict a-priory practical aspects of the current and new multiple-access wireless communication networks, such as: the users' capacity and user's links spectral efficiency for various configurations of cells deployment — femto, pico, micro, and macro, as well as the novel MIMO/LTE system configuration for future networks of 4th and 5th generation deployment.*

Keywords *— capacity, multiple-input-multiple-output (MIMO), MIMO channel, spectral efficiency, K-factor, space-time diversity, spatial multiplexing urban environment, dense layout of buildings.*

Citation: Sergeev A. M., Blaunstein N. Sh. Evolution of multiple-access networks — cellular and non-cellular — in historical perspective. Part 2. *Informatsionno-upravliaiushchie sistemy* [Information and Control Systems], 2018, no. 5, pp. 94–103. doi:10.31799/1684-8853-2018-5-94-103

Continuation.
Start in *Informatsionno-upravliaiushchie sistemy* [Information and Control Systems], 2018, no. 4, pp. 86–104.
doi:10.31799/1684-8853-2018-4-86-104

MIMO modern networks design in the space and time domains

We will now present some advanced technology concepts based on adaptive multi-beam or phased-array antenna applications through the prism of the physical layer description accounting for the "reaction" of the multipath outdoor channel with fading on radio propagation within such a channel [22, 49–62]. These techniques are fully described in references [63–82].

Multiple-input-multiple-output (MIMO) communication systems with multi-beam or multiple-element antennas arranged at both ends of the communication link have been introduced during the last decade to increase of spectral efficiency and communication link reliability that can be achieved via spatial and time diversity techniques. In Fig. 11 is shown an example of how to arrange multibeam antennas (4×4 beams, i. e., 16 beams) that manage and control many clients servicing via the mobile/stationary broadband internet or sensors' networking.

In modern MIMO systems, the two basic techniques usually used [63–82] to mitigate multipath fading phenomena and increase efficiency of such networks, are:

— spatial multiplexing as a space-time modulation techniques;

— diversity modulation technique as a special case of a space-time modulation technique.

According to the first procedure, each transmitting antenna element sends to the receiver *independent* (e. g. non-correlated) streams of signal data accounting for a strong multipath phenomenon occurring in each channel with the Rayleigh fading [63, 64] caused by multiple reflection and diffrac-

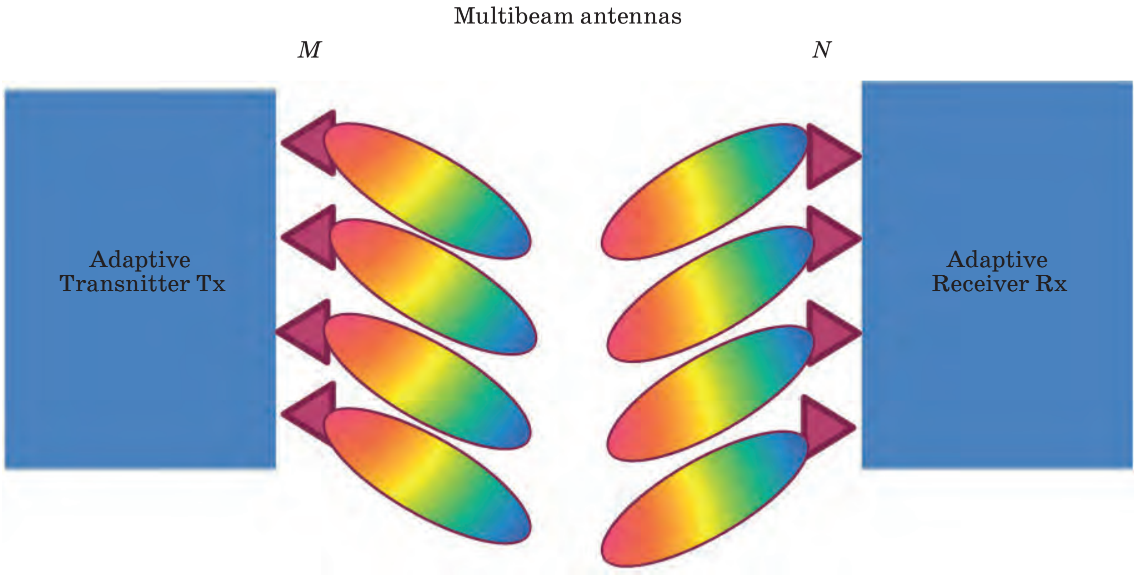

■ ***Fig. 11.*** MIMO system based on $M \times N$ multibeam antennas

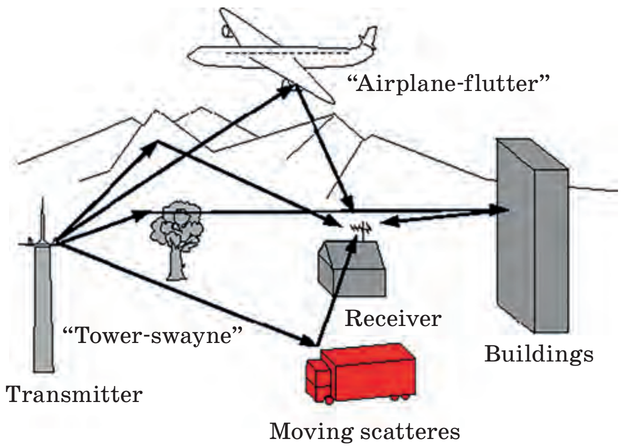

■ ***Fig. 12.*** Schematically presented effects of multiray phenomena occurring in the real wireless MIMO channel that causes strong fading on the input/output signals

tion occurring in the real wireless environment (Fig. 12). This idea of spatial multiplexing was first proposed in Reference [47], which then was adapted in practice of MIMO systems deployment in [66, 67]. Initially spatial multiplexing systems used narrowband channel for each antenna element of the MIMO system with a small delay spread (i. e., the large bandwidth of coherency B_{cn}, see previous section). In modern MIMO systems spatial multiplexing was adapted for wideband channels too in conjunction with OFDM modulation technique [68–72].

In contrast to spatial multiplexing, the diversity modulation technique deals with *dependent* (e. g. correlated) streams of data from each transmit antenna element of desired MIMO system. There are several diversity modulation techniques, which can be found in references [73–77]. In this book, will be using the term MIMO diversity technique that combines space-time diversity and spatial-time multiplexing according to references [78–82].

Following the results obtained in [22], we will describe the MIMO system capacity, as an example of space-diversity and time-diversity techniques adapted for the use of the multibeam (e. g., multielement) antennas in various built-up environments. For this case, the desired formulas according to the unified multiparametric stochastic approach described in [21, 22, 95–102], will be rearranged to obtain simple relations between the MIMO antenna element number and the parameters of the terrain.

The spectral efficiency of the MIMO technique strongly depends on the diversity among multiple channels which is determined by the spatial statistical behavior of the MIMO fading channel, partly characterized by the special spatial fading correlation function (or coefficients) described in [22]. It was shown in [22, 49–55] that a sufficiently high diversity in the received multipath replicas of the transmitted signal can be achieved within a "rich" scattering environment where the communication channel capacity linearly increases with the number of the transmitter and the receiver antennas. Moreover, [49] was shown that the spatial fading correlation coefficient for *dependent* data streams (or de-correlation coefficient for *independent* data streams) can be determined by the system parameters, such as antenna elements spacing and their number. At the same time, this coefficient can be determined by the propagation conditions, such as the received energy spread in the AOA (angle-of-arrival), TOA (time-of-arrival) and Doppler domains, as it is described in [21, 22].

In practice, scattering environment is a scenario-dependent and as a result, spatial de-correlation characteristics are also scenario dependent [22, 49–52, 55]. Therefore, an accurate modeling of the spatial de-correlation characteristics of the MIMO channels is crucial for investigation of the scenario-specific spectral efficiency, which serves as the main criterion for communication systems design and wireless networks planning. Thus, we will derive the MIMO channel capacity for various propagation conditions as a function of the spatial correlation and the received distribution in the AOA-TOA domain. The proposed spatial fading correlation will be introduced via the stochastic multiparametric model of the urban propagation conditions in a joint AOA-TOA domain described in [21, 22, 50–52]. As a result of the proposed stochastic approach, it can be shown that the spatial fading correlation parameters depend on the propagation phenomena, such as multiple scattering, reflection, diffraction, as well as on the waveguide propagation along streets, which characterize urban environment propagation conditions.

Modeling of MIMO channel capacity

Usually, as follows from Fig. 11, there are several output antennas and input antennas assembled at the transmitter and the receiver, which we will denote them by M and N respectively.

For the uncorrelated antennas (e. g. working as separate independent antenna elements) arranged at the MIMO channel, the spectrally normalized to bandwidth B_w [in Hz] capacity C [e. g., *spectral efficiency* measured in bit/s/Hz] was defined in [50] as

$$\tilde{C}_{\text{uncorr}} = = N\log_2\left(\left(K_m \cdot \left(\frac{P_m}{N}\right)_{\text{add}}\right)\Big/\left(K_m + \left(\frac{P_m}{N}\right)_{\text{add}}\right)\right), \quad (26a)$$

where $(P_m/N)_{\text{add}}$ is the signal to additive Gaussian noise ratio, which usually is taken into account in the literature. We also accounted the multiplicative noise caused by fading multipath phenomena, occurring in each of N input channels, where Km = (LOS-component)/(Multipath-component) — is the ratio of the coherent (e. g., deterministic) component of the signal and incoherent (stochastic) component of the signal caused the multiplicative noise.

At the same time, for the case of correlated antennas (i. e., working as unified whole transmitter and receiver antenna) the spectral efficiency [measured in bit/s/Hz] can be presented according to [50] as

$$\tilde{C}_{\text{corr}} = \log_2\left(1 + MN\left(K_m \times \times\left(\frac{P_m}{N}\right)_{\text{add}}\right)\Big/\left(K_m + \left(\frac{P_m}{N}\right)_{\text{add}}\right)\right). \quad (26b)$$

Thus, mentioned above can be proved by a special numerical simulations carried out for different values of SNR = $(P_m/N)_{\text{add}}$ [in dB], and for various amounts of elements M and N at the transmitter (output) and receiver (input) antennas, respectively. We should notice before presenting some results of numerical computations that the uncorrelated arrangement of the MIMO antenna elements at the both terminal sides allows to obtain much higher capacity, e. g., higher spectral efficiency of each M and N channels with respect to the case of the correlated arrangement of the antenna elements into the unique antenna. This can be clearly seen from formulas (26a) and (26b), where in (26a) the number of elements at the receiver N is outside the logarithmic function and C increases linearly with increase of elements N at the input of the receiver. At the same time, in (26b) N and M are inside the logarithm, that is, capacity and the spectral efficiency increases logarithmically (i. e., very slow) with increase of number of elements N and M. In [50, 51] are presented several variants of MIMO system arrangements to proof mentioned above. Therefore, we will present here only the case of the uncorrelated arrangement of the antenna elements, M and N. Thus, Fig. 13 presents a spectral efficiency vs. the fading factor K, as a ratio of the coherent and incoherent (multipath) components of the signal at the input of the multi-element (M = 2) transmitter antenna and multi-element (N = 4) receiving antenna, according to scenario shown in Fig. 12.

As clearly seen from the presented illustration, with increase of the coherent component (e. g. line-of-sight component) of the income signals at the input of the multi-element receiver antenna with respect to the multipath component (caused by multi-diffraction and multi-scattering from obstruc-

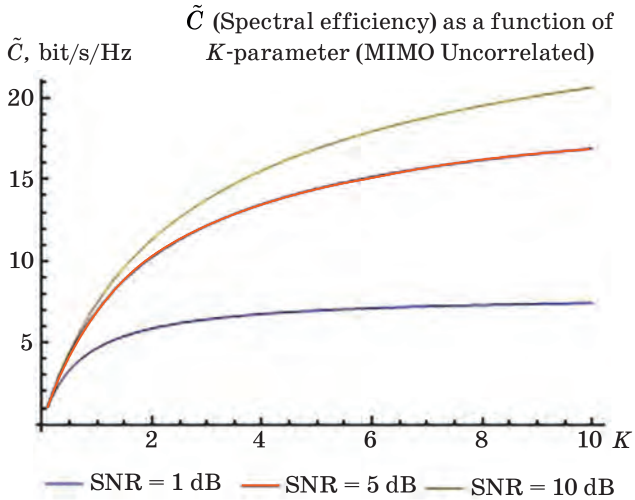

■ ***Fig. 13.*** Spectral efficiency vs. the K-parameter of fading for various values of signal to additive noise ratio for M = 2 and N = 4 tions located in area of users' service), that is, with increase of K-factor of fading, the spectral efficiency increases sharply till K~4÷6, and then a saturation of the process becomes evident.

This effect depends on SNR and becomes for smaller (K~2) with increase of SNR from 1 to 10 dB. In other words, increasing SNR inside the MIMO system, it can be easier to obey effect of fading caused by real conditions of each land-to-land communication channel.

Considering now, according to [51], the uplink scenario where the multiple receiving antennas in the BS are spatially separated, the correlation among the received replicas of the transmitted signal is determined by the propagation conditions and the spatial separation distance, that is,

$$\rho = \int_0^{2\pi} e^{ikr\sin(\varphi)} f(\varphi)\mathrm{d}\varphi, \qquad (27)$$

where $k = 2\pi/\lambda$ is a wavenumber, λ is a wavelength; r is a spatial spacing between the transmitter or the receiver antennas, which in practice is limited by the physical dimensions of the platform or installation constraints; φ is AOA; $f(\varphi)$ is an angular spectrum. Conventionally it is assumed that $M > N$.

The influence of the MIMO channel correlation, represented by the transmitter and the receiver spatial correlation matrices on the channel capacity is intensively studied in the literature (see [22, 49–51, 53]). Following [50, 51], we will represent the influence of the spatial fading correlation in (27) on the MIMO channel capacity in (26) in the more convenient and simple manner to understand the matter:

$$\tilde{C} = N\log_2\left(1 + (1-\rho)\frac{M}{N}\frac{SNR}{B_w}\right). \qquad (28)$$

Notice that the spatial fading correlation in (28) decreases the MIMO channel capacity. Moreover, as was shown in addition, note that the received energy spread in the AOA-TOA domain is inversely proportional to the correlation and therefore directly proportional to the achievable channel capacity. Thus, the higher received signal spread is represented by a smaller correlation, $\rho \to 0$, which results in a higher MIMO channel capacity according to equation (28).

Fading correlation in space-time doman in urban environment with complicated building layout

considering the below-the-rooftops propagation conditions [51], and using the corresponding formulas presented in [22], the fading correlation in (26) can be rewritten as follows:

$$\rho_{\text{below}} = \int_0^{2\pi} f_{\text{below}}(\varphi) e^{jkd\sin\varphi}\mathrm{d}\varphi, \qquad (29)$$

where

$$f_{\text{below}}(\varphi) = \int_{\tau=0}^{t}\left(\frac{\bar{L}\nu^2\tau d^2(\tau^2-1)}{2\pi(\tau-\cos\varphi)}\beta(\varphi)e^{-\frac{2\bar{L}\nu\tau d}{\pi}}\right)\times$$
$$\times e^{\left(-\frac{d(\tau^2-1)|\ln\chi|}{(\tau-\cos\varphi)a'(\varphi)}\right)}\mathrm{d}\tau, \qquad (30)$$

where d is the straight-line distance between the MS (mobile subscriber) and the BS, km; τ is the ratio between the actual distance that signal travels from the MS to the BS and d; φ is the AOA; ν is the building density per square km [i. e., in km^{-2}];

$$\beta(\varphi) = \sin^2\left(\frac{1}{2}\arcsin\left(\frac{d\sin(\varphi)}{\tilde{r}}\right)\right),$$

$\chi = \bar{L}/(\bar{L}+\bar{l})$ is the street "discontinuity" parameter, where $\bar{L}$ is the average lengths of the buildings, km; $\bar{l}$ is the average lengths of the slits (gaps) between the buildings, km; $a' = \sqrt{\frac{4a^4}{\lambda^2 n^2} + a^2}$, where a is the average width of streets, km, and n is the street waveguide mode number.

Considering wave propagation above the rooftops, and using formulas derived in [22], the correlation coefficient in (26) can be obtained as follows [51]:

$$\rho_{\text{above}} = \int_0^{2\pi} f_{\text{above}}(\varphi) e^{jkd\sin\varphi}\mathrm{d}\varphi, \qquad (31)$$

where

$$f_{\text{above}}(\varphi) = \int_{\tau=0}^{t}\left[\frac{\bar{L}\nu^2\tau d^2(\tau^2-1)}{2\pi(\tau-\cos\varphi)}\times\right.$$
$$\times\beta(\varphi)\frac{\bar{h}}{h_R}e^{-\frac{2\bar{L}\nu}{\pi}\left(\tilde{r}(\tau,\varphi)+\frac{\bar{h}}{h_R}\frac{d(\tau^2-1)}{2(\tau-\cos\varphi)}\right)}+$$
$$\left.+\frac{\nu}{2}\beta(\varphi)\frac{(h_R-\bar{h})\tilde{r}(\tau,\varphi)}{\bar{h}}e^{-\frac{2\bar{L}\nu\tilde{r}(\tau,\varphi)}{\pi}}\right]\times$$
$$\times e^{\left(-\frac{d(\tau^2-1)|\ln\chi|}{(\tau-\cos\varphi)a'(\varphi)}\right)}\mathrm{d}\tau, \qquad (32)$$

here, assuming a uniform distribution of building heights; $\bar{h} = \frac{h_1+h_2}{2}$ is the average height of building profiles, where h_1 and h_2 are the minimum and maximum building heights; h_R is the BS antenna height, and $\tilde{r}(\tau,\varphi)=\dfrac{d(\tau^2-2\tau\cos\varphi+1)}{2(\tau-\cos\varphi)}$. Below, we will analyze MIMO channel capacity in specific urban scenarios.

Correlation coefficient analysis in urban scene

The spatial fading correlation is analyzed in various urban propagation conditions simulated by the proposed f_{below} and f_{above} models according to (30) and (32), respectively. Following [51], we analyse an urban environment with the following parameters of the experiment described there: the two BS receiving antennas with a separation distance of $\frac{r}{\lambda}=10$ located in the urban scene with the following parameters: $\gamma_0=8$ km^{-1}, $\chi=0.5$, $d=0.3$ km, pseudo-LOS is at $\varphi=0°$, $\bar{h}=\dfrac{h_1+h_2}{2}=15$ m, $\nu=250$ km^{-2}. Figure 14 shows the correlation coefficient ρ from (32) as a function of the BS antenna height h_R and the buildings' density parameter, $\gamma_0=\dfrac{2\bar{L}\nu}{\pi}$, which describes the clutter density in urban scenario.

As follows from results presented in Fig. 14, the spatial fading correlation is directly proportional to the BS antenna height. We can outline that the results shown in Fig. 14 agree with those obtained in [52, 55]. In addition, Fig. 14 shows that the spatial fading correlation is inversely proportional to the buildings' density parameter, γ_0 (e. g., *clutter* density), which determines the received signal diversity in the AOA-TOA domain. Therefore, the denser urban environment (higher γ_0) results in lower correlation among the received replica of the transmitted signal. Finally, we notice that the influence of the parameter γ_0 on the spatial fading correlation decreases with increasing BS antenna height. This observation can be explained by the fact that the significance of the built-up environment structure for a particular urban scene (distribution of the scatterers) decreases with increasing BS antenna height. In practice, the result shown in Fig. 14 can be used as a guideline for the BS antenna height selection required to achieve the predefined correlation (and as a result the predefined MIMO channel capacity) in a specific urban scenario.

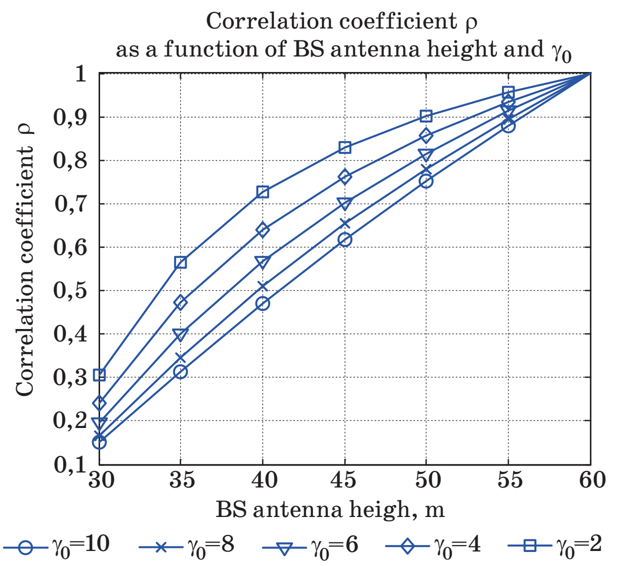

■ ***Fig. 14.*** Correlation coefficient vs. the BS antenna height h_R for various $\gamma_0=2, 4, 6, 8, 10$ km^{-1} in the urban environment with $r=10\lambda$, $\chi=0.5$, $d=0.3$ km, pseudo-LOS is at 0°, $\bar{h}=15$ m, $\nu=250$ km^{-2}

MIMO channel capacity estimation

Now, we will analyze the effect of the spatial fading correlation on the MIMO channel capacity by using (29) and (31) in (32). In Fig. 15, ***a*** shows the MIMO channel capacity as a function of the BS antenna heights for a variety of the buildings' density γ_0 in the simulated urban environment with the following parameters: SNR = 10 dB, separation distance between two BS receiver antennas of $r=10\lambda$, $\chi=0.5$, $d=0.5$ km, pseudo LOS is at $\varphi=0°$, and $\bar{h}=25$ m.

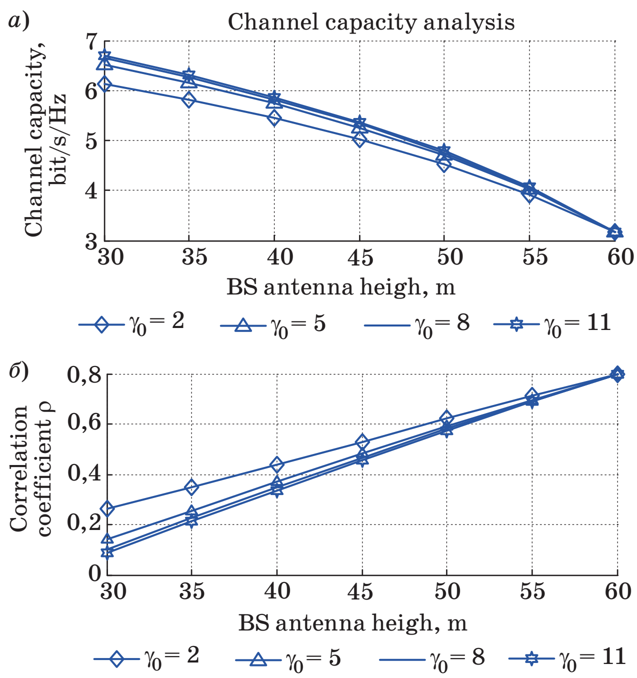

■ ***Fig. 15.*** MIMO channel capacity vs. the correlation coefficient and γ_0 in the urban scenario with SNR = = 10 dB, $r/\lambda=10$, $\chi=0.5$, $d=0.5$ km, pseudo LOS is at $\varphi=0°$, and $\bar{h}=25$ m

We show that the MIMO channel capacity in Fig. 15, *a*, to be inversely proportional to the spatial fading correlation in Fig. 15, *b*. Thus, the increase in the spatial fading correlation ρ from 0.2 to 0.8 results in the normalized channel capacity degradation from approximately 6.5 bit/s/Hz to approximately 3.2 bit/s/Hz.

Notice that the MIMO channel capacity is directly proportional to the buildings' density γ_0 in the urban environment. Thus, the increase in the density γ_0 from 2 to 11 km^{-1}, results in the channel capacity improvement.

This simulations show that in additional to the conventional dependence of the MIMO channel capacity on SNR, it strongly depends on the location-specific parameters of the urban environment (via the statistical model of the urban propagation conditions), such as BS antenna height, buildings' density, average buildings' height, and so forth.

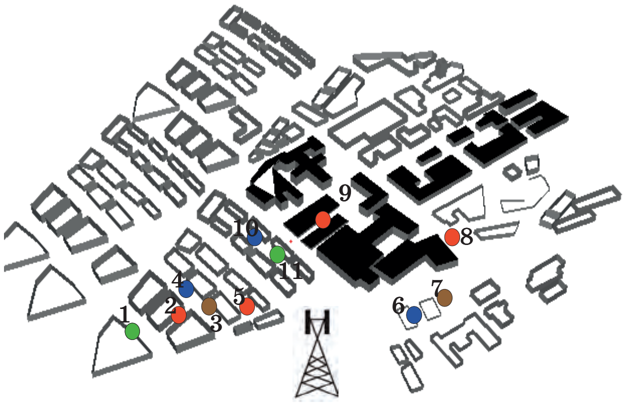

■ ***Fig. 16.*** The MIMO channel capacity is simulated urban scenario with the BS antenna height of 15 m, MIMO system is with 4 × 4 antenna elements, and SNR = 20 dB; the numbers show places where numerical experiment was carried out

MIMO channel capacity analysis in predefined urban scenario

Now we will evaluate the MIMO channel capacity in a simulated "virtual" urban scenario, using an urban topographic plan taken from [22, 51]. The MIMO channel capacity was evaluated in 11 representative locations characterized by the SNR of 20 dB. The SNR was obtained using the ray-tracing software tool [54] as a ratio between the received signal strength and the noise with an equivalent bandwidth of 5 MHz. A BS antenna height of 15 m was simulated. The separation distance of $r = 10\lambda$ was simulated between 4 receiving antennas. The urban environment with the following parameters was simulated using (30) and (32): $\chi = 0.8$, $\bar{h} = 25$ m, $\gamma_0 = 6$ km^{-1}. The inter-user interference was neglected in this simulation.

Figure 16 shows the simulated urban scene. Colored dots in Fig. 16 show the tested MS locations with the SNR of 20 dB. The color pattern represents the achievable 4 × 4 MIMO channel capacity. Numbers near each color circle, from 1 to 9, indicate position of the MS antenna with respect to the BS antenna, shown in the picture, during the computer experiment. Notice that different locations (with equal SNR) are characterized by different spatial fading correlation and therefore the resulting MIMO channel capacity varies among these locations. We also notice that results shown in Fig. 16 agree with the results obtained during the measurement reported in references [45, 55].

The above obtained results allow us to summarize that the MIMO channel capacity in an urban environment has the BS antenna elevation and location specific factor and strongly depends on the spatial fading correlation determined by the scattering, reflection, diffraction and waveguide propagation phenomena.

To be continued.

References

1. **Jakes W. C.** *Microwave Mobile Communications.* Wiley, New York, 1974.
2. **Lee S. C. Y.** *Mobile Cellular Telecommunication Systems*. McGraw-Hill, New York, 1989.
3. **Steele R.** *Mobile Radio Communication*. IEEE Press, 1992.
4. **Proakis J. G.** *Digital Communications*. 3d ed. McGraw-Hill, New York, 1995.
5. **Stuber G. L.** *Principles of Mobile Communications.* Kluwer Academic Publishers, Boston, 1996.
6. **Peterson R. L., Ziemer R. E., and Borth D. E.** *Introduction to Spread Spectrum Communications*. Prentice Hall PTR, New Jersey, 1995.
7. **Rappaport T. S.** *Wireless Communications: Principles and Practice*. Prentice Hall PTR, New Jersey, 1996; (2nd ed.) in 2001.
8. **Steele R., and Hanzo L.** *Mobile Communications.* 2nd ed. John Wiley & Sons, Chickester, 1999.
9. **Li J. S., and Miller L. E.** *CDMA Systems Engineering Handbook*. Artech House, Boston-London, 1998.
10. **Saunders S. R.** *Antennas and Propagation for Wireless Communication Systems.* John Wiley& Sons, Chickester, 2001.
11. **Burr A.** *Modulation and Coding for Wireless Communications*. Prentice Hall PTR, New Jersey, 2001.
12. **Molisch A. F. (Ed.).** *Wideband Wireless Digital Communications*. Prentice Hall PTR, New Jersey, 2000.

13. **Paetzold M.** *Mobile Fading Channels: Modeling, Analysis, and Simulation*. John Wiley & Sons, Chickester, 2002.
14. **Simon M. K., Omura J. K., Scholtz R. A., and Levitt B. K.** *Spread Spectrum Communications Handbook*. McGraw-Hill, New York, 1994.
15. **Glisic S. and Vucetic B.** *Spread Spectrum CDMA Systems for Wireless Communications*. Artech House, Boston-London, 1997.
16. **Dixon R. C.** *Spread Spectrum Systems with Commercial Applications*. John Wiley & Sons, Chickester, 1994.
17. **Viterbi A. J.** *CDMA: Principles of Spread Spectrum Communication*. Addison-Wesley Wireless Communications Series, 1995.
18. **Goodman D. J.** *Wireless Personal Communication Systems*. Addison-Wesley, Reading, Massachusetts, 1997.
19. **Schiller J.** *Mobile Communications*. 2nd ed. Addison-Wesley Wireless Communications Series, 2003.
20. **Molisch A. F.** *Wireless Communications*. John Wiley & Sons, Chickester, 2007.
21. **Blaunstein N. and Christodoulou C.** *Radio Propagation and Adaptive Antennas for Wireless Communication Links*. 1st ed. Wiley & Sons, New Jersey, 2007.
22. **Blaunstein N. and Christodoulou C.** *Radio Propagation and Adaptive Antennas for Wireless Communication Networks — Terrestrial, Atmospheric and Ionospheric*. 2nd ed. Wiley & Sons, New Jersey, 2014.
23. **Hadar O., Bronfman I., and Blaunstein N.** Optimization of Error Concealment Based on Analysis of Fading Types. Part 1. Statistical Description of the Wireless Video Channel, Models of BER Determination and Error Concealment of Video Signals. *Informatsionno-upravliaiushchie sistemy* [Information and Control Systems], 2017, no. 1, pp. 72–82. doi:10.15217/issn1684-8853.2017.1.72
24. **Hadar O., Bronfman I., and Blaunstein N.** Optimization of Error Concealment Based on Analysis of Fading Types. Part 2. Modified and New Models of Video Signal Error Concealment. Practical Simulations and their Results. *Informatsionno-upravliaiushchie sistemy* [Information and Control Systems], 2017, no. 2, pp. 67–76. doi:10.15217/issn1684-8853.2017.2.67
25. **Vostrikov A., Kurtyanik D., Sergeev A.** Choosing Embedded WI-FI Module for Mobile Optic-Information Systems. *Vestnik*, 2018, no. 4, pp. 26–29 (In Russian).
26. **Vostrikov A., Balonin Yu., Kurtyanik D., Sergeev A., Sinitsyna O.** On Hybrid Method of Video Data Protection in IP-networks. *Telekommunikatsii* [Telecommunications], 2018, no. 2, pp. 34–39 (In Russian).
27. **Erosh I., Sergeev A., Filatov G.** Protection of Images During Transfer via Communication Channels. *Informatsionno-upravliaiushchie sistemy* [Information and Control Systems], 2007, no. 5, pp. 20–22 (In Russian).
28. **Sergeev A.** Generalized Mersenne Matrices and Balonin's Conjecture. *Automatic Control and Computer Sciences*, 2014, vol. 48, no. 4, pp. 214–220.
29. **Sergeev A. M., Blaunstein N. S.** Orthogonal Matrices with Symmetrical Structures for Image Processing. *Informatsionno-upravliaiushchie sistemy* [Information and Control Systems], 2017, no. 6, pp. 2–8 (In Russian). doi:10.15217/issn1684-8853.2017.6.2
30. *Modulation and Coding Techniques in Wireless Communications*. Ed. by Krouk E., and Semenov S. John Wiley & Sons, Chichester, United Kindom, 2011.
31. *Specification of the Bluetooth System*. Dec. 1, 1999. Available at: www.bluetooth.com. (accessed 15 August 2017).
32. **Junaid M., Mufti M., and Ilyas M. U.** Vulnerabilities of IEEE 802.11i Wireless LAN. *Trans. Eng., Comput. and Technol.*, Feb. 2006, vol. 11, pp. 228–233.
33. *IEEE 802.11 Working Group*. Available at: http://grouper.ieee.org/groups/802/11/index.html (accessed 15 August 2017).
34. *Wireless Ethernet Compatibility Alliance*. Available at: http://www.wirelessethernet.org/index.html (accessed 15 August 2017).
35. **Sharon O., and Altman E.** An Efficient Polling MAC for Wireless LANs. *IEEE/ACM Trans. on WiMAX Systems Evaluation Methodology V2.1etworking*, 2001, vol. 9, no. 4, pp. 439–451.
36. IEEE std. 802.11-1999: *Wireless LAN Medium Access Control* (*MAC*) *and Physical Layer* (*PHL*) *Specifications*, 1999.
37. **Qainkhani I. A., and Hossain E.** A Novel QoS-aware MAC Protocol for Voice Services over IEEE 802.11-based WLANs. *J. Wireless Communic. and Mobile Comput.*, 2009, vol. 9, pp. 71–84.
38. *Wireless LAN Medium Access Control and Physical Layer Specification*. IEEE Press, 1999, Jan. 14.
39. **Zyren J.** *Reliability of IEEE 802.11 High Rate DSSS WLANs in a High Density Bluetooth Environment*; 802.11 section, 8–6, 1999.
40. **Perahia E.** IEEE 802.11n Development: History, Process, and Technology. *IEEE Communic. Magazine*, 2008, vol. 46, pp. 46–55.
41. **Ni Q., Romshani L., and Turletti T.** A Survey of QoS Enhancements for IEEE 802.11 Wireless LAN. *J. Wireless Communic. and Mobile Comput.*, 2004, vol. 4, no. 5, pp. 547–566.
42. **Wang W., Liew S. C., and Li V. O. K.** Solutions to Performance Problems in VoIP over 802.11 Wireless LAN. *IEEE Trans. Veh. Tech.*, 2005, vol. 54, no. 1, pp. 366–384.
43. **Robinson J. W., and Randhawa T. S.** Saturation Throughput Analysis of IEEE 802.11e Enhanced Distributed Coordination Function. *IEEE J. Select. Areas of Communic.*, 2004, vol. 22, no. 5, pp. 917–928.
44. **Wang P., Jiang H., and Zhuang W.** 802.11e Enhancement for Voice Service. *IEEE Wireless Communic.*, 2006, vol. 13, no. 1, pp. 30–35.
45. **Perez-Costa X., and Camps-Mur D.** IEEE 802.11e QoS and Power Saving Features Overview and Analysis of Combined Performances. *IEEE Wireless Communic.*, 2010, vol. 17, no. 2, pp. 88–96.

46. **Kopsel A., and Wolisz A.** Voice Ptransmission in an IEEE 802.11 WLAN Based Access Network. *Proc. of 4th ACM Int. Workshop on Wireless Mobile Multimedia (WoWMoM)*, Rome, Italy, 2001, pp. 24–33.
47. **Veeraraghavan M., Chocker N., and Moors T.** Support of Voice Services in IEEE 802.11 Wireles LANs. *Proc. of IEEE INFOCOM'01*, 2001, vol. 1, pp. 488–497.
48. **Kim Y-J., and Suh Y-J.** Adaptive Polling MAC Schemes for IEEE 802.11 Wireless LANs Supporting Voice-over-IP (VoIP) Services. *J. Wireless Communic. and Mob. Comput.*, 2004, vol. 4, pp. 903–916.
49. **Andersen J. B.** Array Gain and Capacity of Known Random Channels with Multiple Element Arrays at Both Ends. *IEEE J. Selected Areas in Coomun.*, 2000, vol. 18, pp. 2172–2178.
50. **Blaunstein N., and Yarkoni N.** Capacity and Spectral Efficiency of MIMO Wireless Systems in Multipath Urban Environment with Fading. *Proc. of the European Conf. on Antennas and Propagation*, *EuCAP-2006*, Nice, France, 2006, pp. 111–115.
51. **Tsalolihin E., Bilik I., and Blaunstein N.** MIMO Capacity in Space and Time Domain for Various Urban Environments. *Proc. of 5th European Conf. on Antennas and Propagation, EuCAP*, Rome, Italy, 11–15 April, 2011, pp. 2321–2325.
52. **Chizhik D., Farrokhi F., Ling J., and Lozano A.** Effect of Antenna Separation on Capacity of BLAST in Correlated Channels. *IEEE Commun. Letters*, 2000, vol. 4, no. 11.
53. **Gesbert D., Shafi M., Shiu D., Smith P., and Naguib A.** From Theory to Practice: An Overview of MIMO Space-Time Coded Wireless Systems. *IEEE Journal on Selected Areas in Comm.*, 2003, vol. 21, no. 3, pp. 281–302.
54. *Radioplan*. RPS user Manual 5.4. Available at: http://www.actix.com (accessed 15 August 2017).
55. **Philippe J., Schumacher L., Pedersen K., Mogensen P., and Frederiksen F.** A Stochastic MIMO Radio Channel Model with Experimental Validation. *IEEE J. Selected Areas in Commun.*, 2002, vol. 20, no. 6, pp. 1211–1226.
56. **Gesbert D., Boleskei H., Gore D. A., and Paulraj A. J.** Outdoor MIMO Wireless Channels: Models and Performance Prediction. *IEEE Trans. Commun.*, 2002, vol. 50, no. 6, pp. 1926–1934.
57. **Boleskei H., Borgmann M., and Paulraj A. J.** On the Capacity of OFDM-based Spatial Multiplexing Systems. *IEEE Trans. Commun.*, 2002, vol. 50, no. 1, pp. 225–234.
58. **Boleskei H., Borgmann M., and Paulraj A. J.** Impact of the Propagation Environment on the Performance of Space-Frequency Coded MIMO-OFDM. *IEEE J. Select. Areas Commun.*, 2003, vol. 21, no. 2, pp. 427–439.
59. **Chizik D., Ling J., Wolniansky P. W., Valenzuela R. A., Costa N., and Huber K.** Multiple-imput-multiple-output Measurements and Modeling in Manhattan. *IEEE J. on Selected Areas in Comm.*, 2003, vol. 23, no. 2, pp. 321–331.
60. **Oyman O., Nabar R. U., Boleskei H., and Paulraj A. J.** Characterizing the Statistical Properties of Mutual Information in MIMO Channels. *IEEE Trans. Signal Processing*, 2003, vol. 51, pp. 2784–2795.
61. **Paulraj A. J., Gore D. A., Nabar R. U., and Boleskei H.** An Overview of MIMO Communications — A Key to Gigabit Wireless. *Proc. of IEEE*, 2004, vol. 92, no. 2, pp. 198–218.
62. **Forenza A.**, et al. Adaptive MIMO Transmission for Exploiting the Capacity of Spatially Correlated Channels. *IEEE Trans. Vehic. Technol.*, 2007, vol. 56, no. 2, pp. 619–630.
63. **Foschini G. J., and Gans M. J.** On Limits of Wireless Communications in a Fading Environment when using Multiple Antennas. *Wireless Person. Communic.*, 1998, vol. 6, no. 3, pp. 311–335.
64. **Proakis J. G.** *Digital Communications*. 4th ed. McGraw-Hill, New York, 2001.
65. **Paulraj A. J., and Kailath T.** *Increasing Capacity in Wireless Broadcast Systems using Distributed Transmission/Directional Reception (DTDR)*. US patent 5,345,599, Sept. 6, 1994.
66. **Foschini G. J.** Layered Space-time Architecture for Wireless Communication in a Fading Environment when using Multiple Antennas. *Bell Labs. Tech. J.*, 1996, vol. 1, no. 2, pp. 41–59.
67. **Golden G. D., Foschini G. J., Valenzula R. A., and Wolniansky P. W.** Direction Algorithm and Initial Laboratory Results using the V-BLAST Space-time Communication Architecture. *Electron. Lett.*, 1999, vol. 35, no. 1, pp. 14–15.
68. **Nabar R. U., Bolcskei H., Erceg V., Gesbert D., and Paulraj A. J.** Performance of Multiantenna Signaling Techniques in the Presence of Polarization Diversity. *IEEE Trans. Signal Process.*, 2002, vol. 50, no. 10, pp. 2553–2562.
69. **Zheng L., and Tse D.** Diversity and Multiplexing: A Fundamental Tradeoff in Multiple Antenna Channels. *IEEE Trans. Inform. Theory*, 2003, vol. 49, no. 5, pp. 1073–1096.
70. **Varadarajan B., and Barry J. R.** The Rate-diversity Trade-off for Linear Space-time Codes. *Proc. IEEE Vehicular Tech. Conf.*, 2002, vol. 1, pp. 67–71.
71. **Godovarti M, and Nero A. O.** Diversity and Degrees of Freedom in Wireless Communications. *Proc. ICASSP*, May 2002, vol. 3, pp. 2861–2864.
72. **Raleigh G. G., and Cioffi J. M.** Spatio-temporal Coding for Wireless Communication. *IEEE Trans. Communic.*, 1998, vol. 46, no. 3, pp. 357–366.
73. **Wittniben A.** Base Station Modulation Diversity for Digital Simulcast. *Proc. IEEE Vehicular Tech. Conf.*, May 1991, pp. 848–853.
74. **Seshadri N., and Winters J. H.** Two Signaling Schemes for Improving the Error Performance of Frequency-Division-Duplex (FDD) Transmission Systems using Transmitter Antenna Diversity. *Int. J.*

Wireless Inform. Networks, 1994, vol. 1, no. 1, pp. 49–60.
75. **Alamouti S. M.** A Simple Transmit Diversity Technique for Wireless Communications. *IEEE J. Select. Areas Communic.*, 1998, vol. 16, no. 8, pp. 1451–1458.
76. **Tarokh V., Seshandri N., and Calderbank A. R.** Space-time Codes for High Data Rate Wireless Communication: Performance Criterion and Code Construction. *IEEE Trans. Inform. Theory*, 1999, vol. 45, no. 5, pp. 1456–1467.
77. **Ganesan G., and Stoica P.** Space-time Block Codes: A Maximum SNR Approach. *IEEE Trans. Inform. Theory*, 2001, vol. 47, no. 4, pp. 1650–1656.
78. **Hassibi B., and Hochwald B. M.** High-rate Codes that are Linear in Space and Time. *IEEE Trans. Inform. Theory*, 2002, vol. 48, no. 7, pp. 1804–1824.
79. **Health Jr., R. W., and Paulraj A. J.** Linear Dispersion Codes for MIMO Systems based on Frame Theory. *IEEE Trans. Signal Process.*, 2002, vol. 50, no. 10, pp. 2429–2441.
80. **Winters J. H.** The Diversity Gain of Transmit Diversity in Wireless Systems with Rayleigh Fading. *IEEE Trans. Veh. Technol.*, 1998, vol. 47, no. 1, pp. 119–123.
81. **Bjerke B. A., and Proakis J. G.** Multiple-antenna Diversity Techniques for Transmission over Fading Channels. *Proc. Wireless Communic. and Networking Conf.*, Sept. 1999, vol. 3, pp. 1038–1042.
82. **Heath Jr., R. W., and Paulraj A. J.** Switching between Diversity and Multiplexing in MIMO Systems. *IEEE Trans. Communic.*, 2005, vol. 53, no. 6, pp. 962–968.
83. **Chandrasekhar V., Andrews J. G., and Gatherer A.** Femtocell Networks: A Survey. *IEEE Commun. Magazine*, 2003, vol. 46, no. 9, pp. 59–67.
84. **Shannon C. E.** A Mathematical Theory of Communication. *Bell System Tech. J.*, July and October 1948, vol. 27, pp. 379–423 and pp. 623–656.
85. **Yeh S.-P., Talwar S., Lee S.-C., and Kim H.** WiMAX Femtocells: A Perpective on Network Architecture, Capacity, and Coverage. *IEEE Commun. Magazine*, 2008, vol. 46, no. 10, pp. 58–65.
86. **Knisely D. N., Yoshizawa T., and Favichia F.** Standardization of Femtocells in 3GPP. *IEEE Commun. Magazine*, 2009, vol. 47, no. 9, pp. 68–75.
87. **Knisely D. N., and Favichia F.** Standardization of Femtocells in 3GPP2. *IEEE Commun. Magazine*, 2009, vol. 47, no. 9, pp. 76–82.
88. **Chandrasekhar V., and Andrews J. G.** Uplink Capacity and Interference Avoidance for Two-tier Femtocell Networks. *IEEE Trans. Wireless Commun.*, 2009, vol. 8, no. 7, pp. 3498–3509.
89. **Calin D., Claussen H., and Uzunalioglu H.** On Femto Deployment Architectures and Macrocell Offloading Benefits in Joint Macro-femto Deployments. *IEEE Commun. Magazine*, 2010, vol. 48, no. 1, pp. 26–32.
90. **Kim R. Y., Kwak J. S., and Etemad K.** WiMAX Femtocel: Requirements, Challenges, and Solutions. *IEEE Commun. Magazine*, 2009, vol. 47, no. 9, pp. 84–91.
91. **Lopez-Perez D., Valcarce A., de la Roche G., and Zhang J.** OFDMA Femtocells: A Roadmap on Interference Avoidance. *IEEE Commun. Magazine*, 2009, vol. 47, no. 9, pp. 41–48.
92. **Chandrasekhar V., Andrews J. G., Muharemovic T., Shen Z., and Gatherer A.** Power Control in Two-tier Femtocell Networks. *IEEE Trans. Wireless Commun.*, 2009, vol. 8, no. 8, pp. 4316–4328.
93. **Yavuz M., Meshkati F., Nanda S.,** et al. Interference Management and Performance Analysis of UMTS/HSPA+Femtocells. *IEEE Commun. Magazine*, 2009, vol. 47, no. 9, pp. 102–109.
94. *Femto Forum*. Available at: http://www.femtoforum.org/femto/ (accessed 15 August 2017).
95. **Blaunstein N. S., and Sergeev M. B.** Channel Capacity Prediction for Femtocell-Macrocell Deployment Strategies in the Urban Environments with Congested Layout of Users. *Informatsionno-upravliaiushchie sistemy* [Information and Control Systems], 2012, no. 3, pp. 54–62 (In Russian).
96. **Tsalolihin E., Bilik I., Blaunstein N., and Babich Y.** Channel Capacity in Mobile Broadband Heterogeneous Networks based on Femto Cells. *Proc. of EuCAP-2012 Int. Conf.*, Prague, Czech Republic, March 26–30, 2012, pp. 1–5.
97. **Blaunstein N., and Levin M.** VHF/UHF Wave Attenuation in a City with Regularly Spaced Buildings. *Radio Science*, 1996, vol. 31, no. 2, pp. 313–323.
98. **Blaunstein N.** Prediction of Cellular Characteristics for Various Urban Environments. *J. Anten. and Propagatat. Magazine*, 1999, vol. 41, no. 6, pp. 135–145.
99. **Blaunstein N.** Average Field Attenuation in the Nonregular Impedance Street Waveguide. *IEEE Trans. on Anten. and Propagat.*, 1998, vol. 46, no. 12, pp. 1782–1789.
100. **Blaunstein N., Katz D., Censor D.,** et al. Prediction of Loss Characteristics in Built-up Areas with Various Buildings' Overlay Profiles. *J. Anten. and Propagat. Magazine*, 2002, vol. 44, no. 1, pp. 181–192.
101. **Yarkoni N., Blaunstein N., and Katz D.** Link Budget and Radio Coverage Design for Various Multipath Urban Communication Links. *Radio Science*, 2007, vol. 42, no. 2, pp. 412–427.
102. **Katz D., Blaunstein N., Hayakawa M., and Kishiki Y. S.** Radio Maps Design in Tokyo City based on Stochastic Multi-parametric and Deterministic Ray Tracing Approaches. *J. Anten. and Propag. Magazine*, 2009, vol. 51, no. 5, pp. 200–208.

УДК 621.371
doi:10.31799/1684-8853-2018-5-94-103

Эволюция многопроцессорных систем связи — сотовых и несотовых — в исторической перспективе. Часть 2

А. М. Сергеев[а], старший преподаватель, orcid.org/0000-0002-4788-9869,
Н. Ш. Блауштейн[б, в], доктор физ.-мат. наук, профессор, nathan.blaunstein@hotmail.com
[а]Санкт-Петербургский государственный университет аэрокосмического приборостроения, Санкт-Петербург, РФ
[б]Негевский университет им. Бен-Гуриона, ПОБ 653, Бен-Гуриона ул., 1, г. Беэр-Шева, 74105, Израиль
[в]Иерусалимский технологический колледж, Хавад Халейми, 21, ПОБ 16031, Иерусалим, 91160, Израиль

Постановка проблемы: целью данного обзора является анализ эволюции систем беспроводной связи от второй генерации (2D) до пятой генерации (5G), а также изменения технологий и их существующих теоретических основ и протоколов — от Bluetooth, WLAN, WiFi и WiMAX до LTE, OFDM/OFDMA, MIMO и LTE/MIMO — продвинутых технологий с новой иерархической структурой дизайна сотовых карт femto/pico/micro/macro. **Методы:** использованы новые теоретические подходы для описания продвинутых технологий, таких как многопользовательская техника разделения пользователей, OFDM и OFDM-новейший подход, новые аспекты описания MIMO-систем на базе использования многолучевых антенн, дизайн различных сотовых карт на основе новых алгоритмов построения фемто/пико/микро/макро сот, а также новой методологии интегрирования новой MIMO/LTE-системы с помощью многолучевых антенн. **Результаты:** создана новая методология описания многопользовательского разделения, использования комбинированной OFDM/OFDMA-модуляции для обхождения интерференции между пользователями и между символами в новых многопроцессорных системах, мультипликативных шумов, имеющих место в беспроводных многопроцессорных системах связи, вызванных явлениями многолучевости. В итоге предложено, как обойти эффекты распространения, имеющие место в наземных каналах связи, используя комбинацию MIMO- и LTE-технологий, основанных на применении многолучевых антенн. Для этих целей разработан новый стохастический подход к проблеме, учитывающий особенности застройки земной поверхности, такие как профиль застройки домов, плотность застройки домов вокруг антенн базовой станции и пользователей и т. д. Эти характеристики позволяют в итоге оценить эффекты фединга как источника мультипликативного шума. **Практическая значимость:** новая методология оценки эффектов, созданных мультипликативным шумом, интерференцией между пользователями и между символами, имеющими место в наземных системах беспроводной связи, позволяет прогнозировать практические аспекты существующих и новых многопроцессорных беспроводных систем связи, такие как емкость (количество) пользователей и спектральная эффективность каналов пользователей для различных конфигураций построения сот — фемто/пико/микро/макро, а также новейших конфигураций систем MIMO/LTE для построения будущих систем 4-го и 5-го поколений.

Ключевые слова — пропускная способность, многочисленный вход-многочисленный выход (MIMO), канал MIMO, пространственное мультиплексирование, спектральная эффективность, фактор *K*, городская среда, плотная застройка домов.

Цитирование: Sergeev A. M., Blaunstein N. Sh. Evolution of multiple-access networks — cellular and non-cellular — in historical perspective. Part 2. *Информационно-управляющие системы*, 2018, № 5, с. 94–103. doi:10.31799/1684-8853-2018-5-94-103
Citation: Sergeev A. M., Blaunstein N. Sh. Evolution of multiple-access networks — cellular and non-cellular — in historical perspective. Part 2. *Informatsionno-upravliaiushchie sistemy* [Information and Control Systems], 2018, no. 5, pp. 94–103. doi:10.31799/1684-8853-2018-5-94-103

К статье
Галининой О. С., Андреева С. Д., Тюрликова А. М.
«Учет специфики доступа большого числа устройств при межмашинном взаимодействии в современных сотовых сетях» («Информационно-управляющие системы», 2018, № 4, с. 105–114.).
На странице 112, правый столбец, последним абзацем вводится дополнение текста:
Исследования Тюрликова Андрея Михайловича выполнены при поддержке гранта РФФИ 17-07-00142 «Разработка моделей и методов анализа надежности соединений в гетерогенных сетях 5G для концепции Интернета надежных вещей».

К статье
Матвеева Н. В., Тюрликова А. М.
«Слотовый ALOHA с итерационной процедурой разрешения коллизий. Стабильность и нестабильность» («Информационно-управляющие системы», 2018, № 3, с. 89–97.).
На странице 96, правый столбец, последним абзацем вводится дополнение текста:
Работа выполнена в рамках инициативного научного проекта № 8.8540.2017/БЧ «Разработка алгоритмов передачи данных в системах IoT с учетом ограничений на сложность устройств».